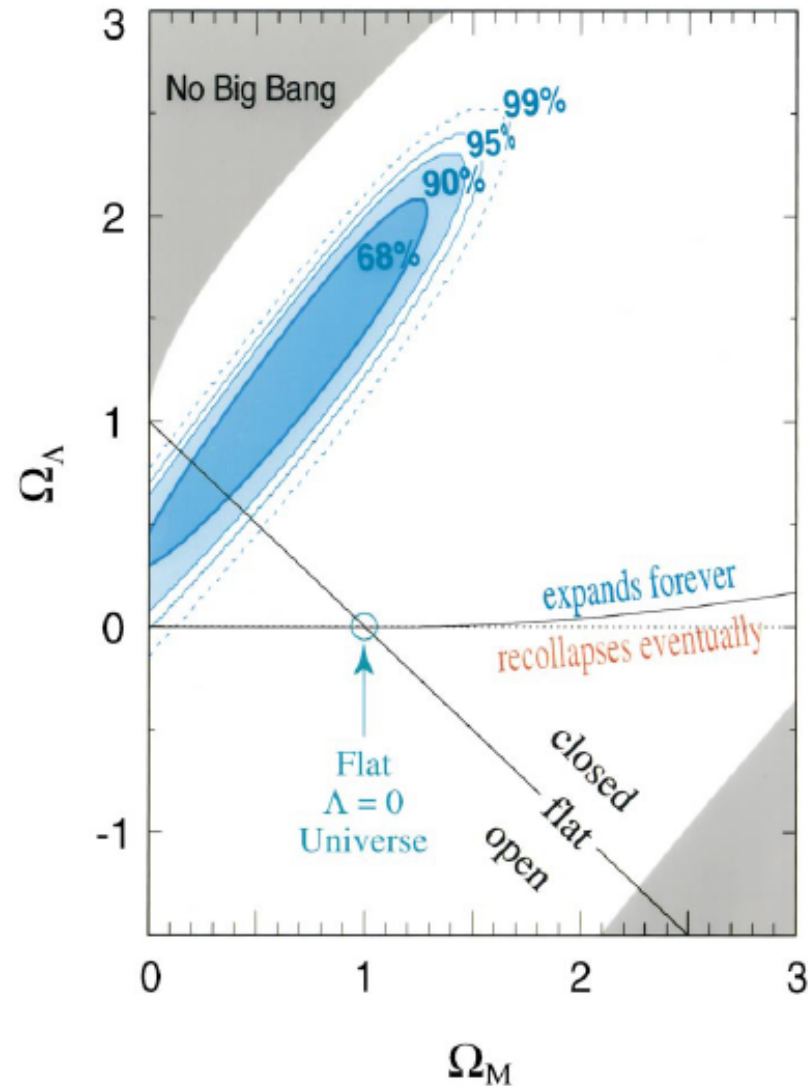


Supernova cosmology in 2014

Pilar Ruiz-Lapuente
IFF (CSIC) & ICC (UB)
Fuerteventura, June 6, 2014

- **Introduction**
- **Type Ia supernovae at z close 2 !**
- **Rising the standard for standard candles (GTC Project also Keck)**
- **Observing SNeIa in the infrared**
- **H_0 from SNeIa**

The Discovery of the Acceleration of the Universe



Best-fit confidence regions in the $\Omega_M - \Omega_\Lambda$ plane. The 68%, 90%, and 99% statistical confidence regions are shown (Perlmutter et al. 1999)

The Discovery of the Acceleration of the Universe

Calibrated candles
through the relation
magnitude- rate of
decline

Pskvoskii-Branch
effect (known in the
80's)

Phillips (1993) Δm_{15}

Riess, Press and
Kirshner (1995)

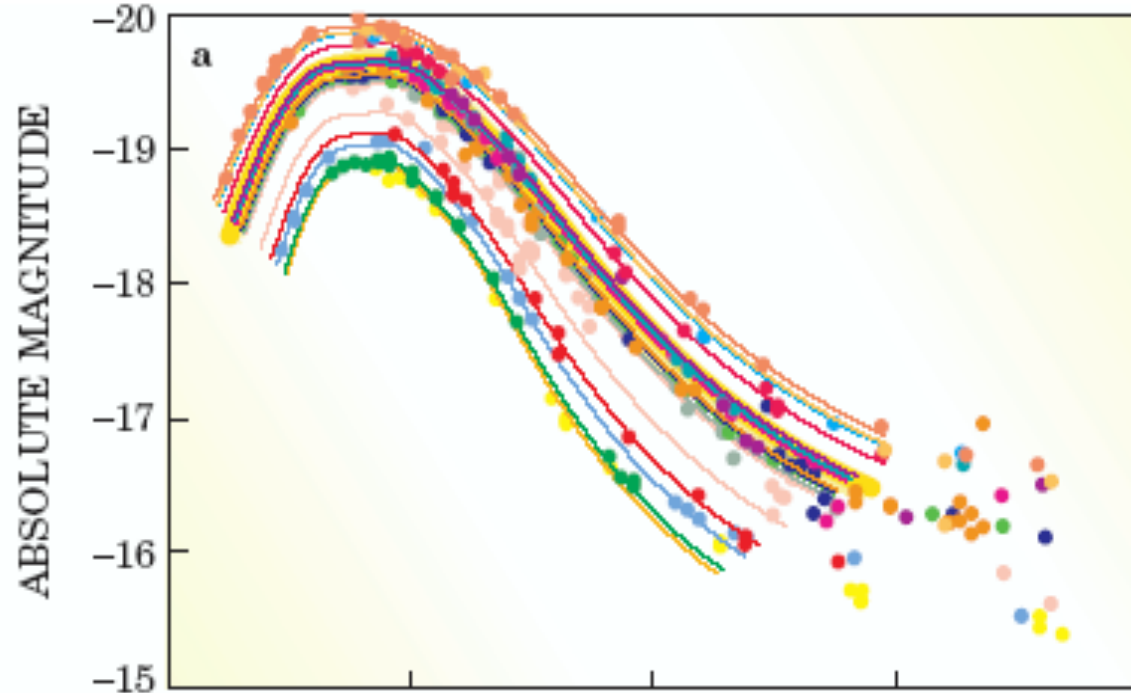
MLCS

Perlmutter et al.
(1996): stretch s

$\sigma \approx 0.15$ mag

With color
information

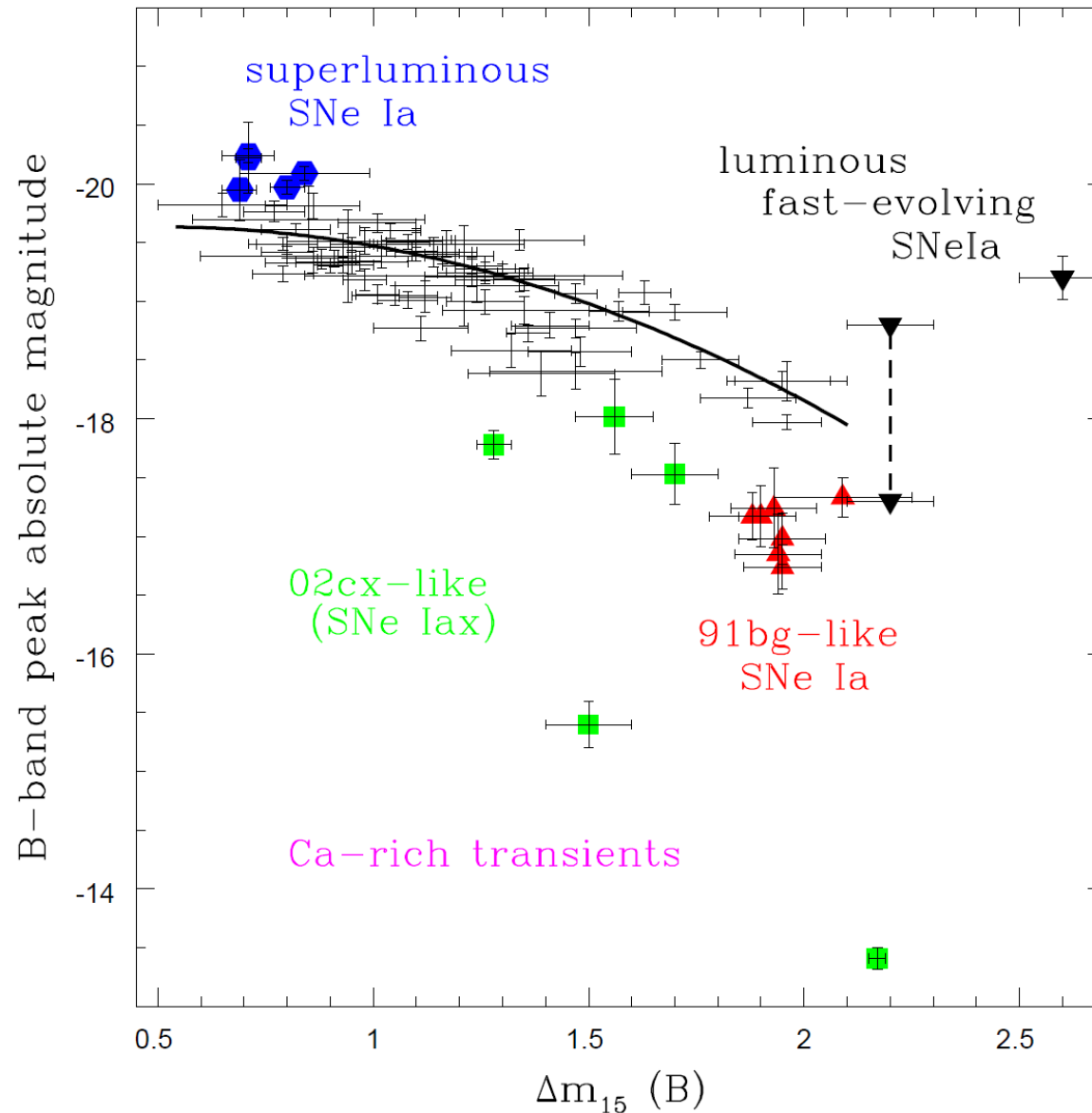
$\sigma \approx 0.11$ mag



The physical Phillips' relation

M_B vs $\Delta m_{15}(B)$

diagram using the CfA3 sample of 185 SNeIa (Hicken et al. 2009). The Phillips et al. (1999) relation is shown by the solid line. The diversity of SNIax is taken from Narayan et al. (2011). The area covered by the Ca-rich transients is marked following Kasliwal et al. (2012). The data on the luminous, fast-evolving SNeIa come from Perets et al. (2011). The very fast SN 2002bj is not shown.



The Discovery of the Acceleration of the Universe

There are three different possible **distance** measurements in Cosmology: from the **brightness** of objects of known luminosity, from the **angular size** of objects of known dimension, and from the **proper** (angular) **motion** of objects traveling with known velocity perpendicularly to the line of sight. Each of them is related to the **redshift** z via the cosmological parameters q , Ω_M , Ω_Λ , and Ω_k . The *luminosity distance*, d_L , is simply defined as

$$d_L \equiv \left(\frac{L}{4\pi f} \right)^{\frac{1}{2}}$$

where L is the luminosity and f the measured flux. As a function of z , H_0 , and q_0

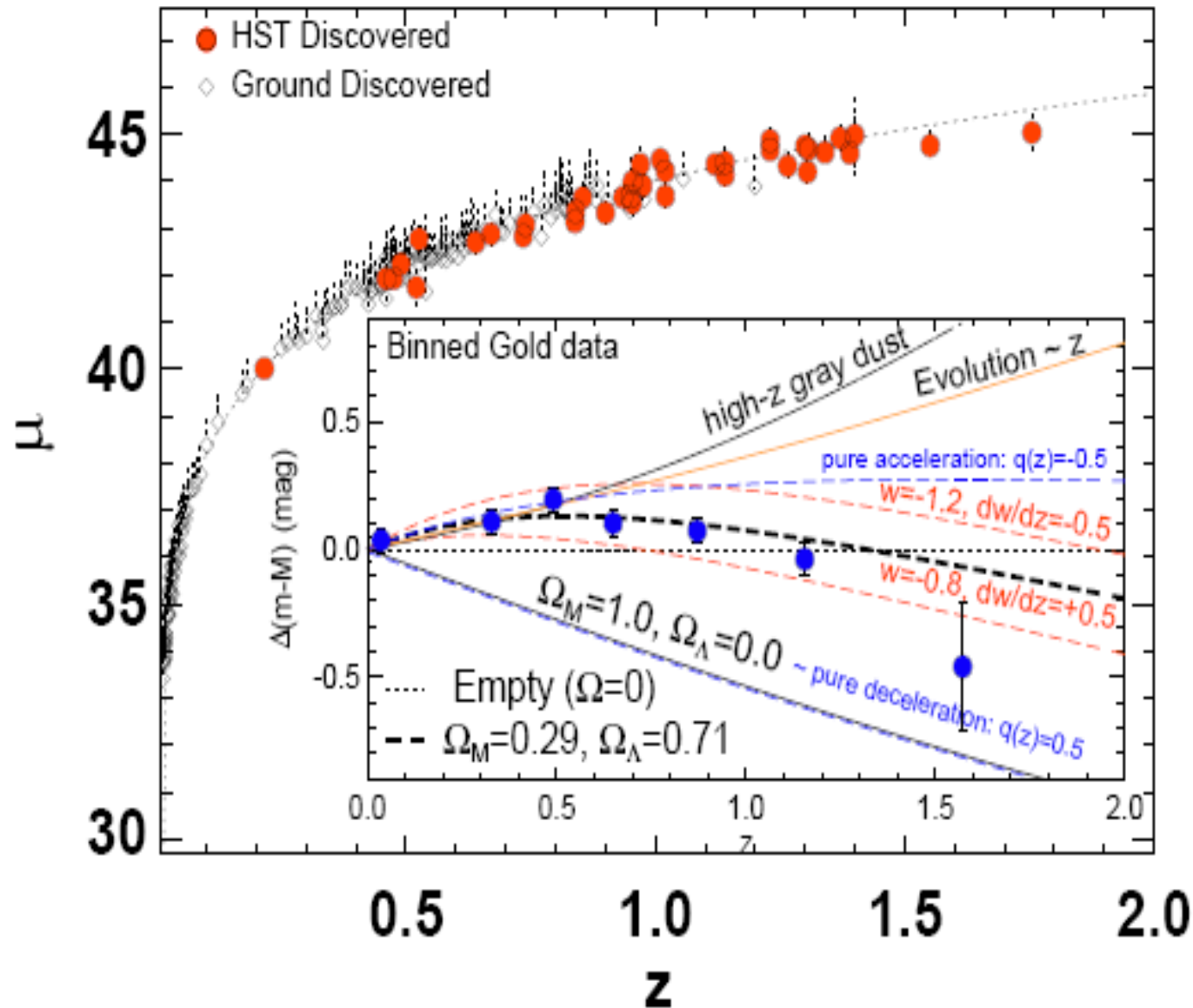
$$H_0 d_L = z + \frac{1}{2}(1 + q_0)z^2 + \dots$$

But more interesting is the full dependence on the three density parameters Ω_M , Ω_Λ , and Ω_k :

$$d_L(z) = cH_0^{-1}(1+z)|\Omega_k|^{-1/2} \text{sinn} \left\{ |\Omega_k|^{1/2} \int_0^z dz' [(1+z')^2(1+\Omega_M z') - z'(2+z')\Omega_\Lambda]^{-1/2} \right\}$$

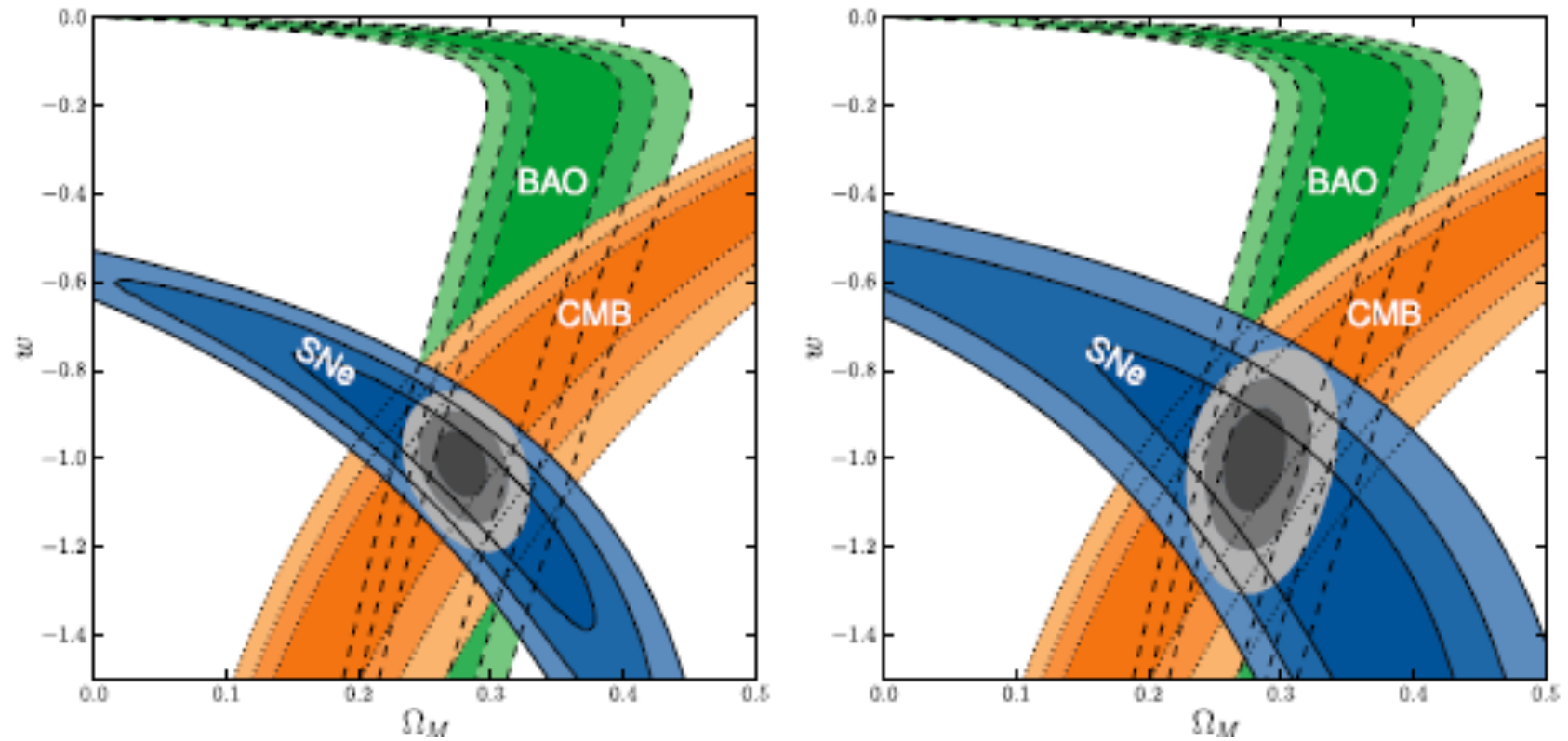
where **sinn**(x) = **sin**(x), **x**, or **sinh**(x) for **closed**, **flat**, and **open** universes, respectively

The Discovery of the Acceleration of the Universe



Riess et al. (2007)

The Discovery of the Acceleration of the Universe

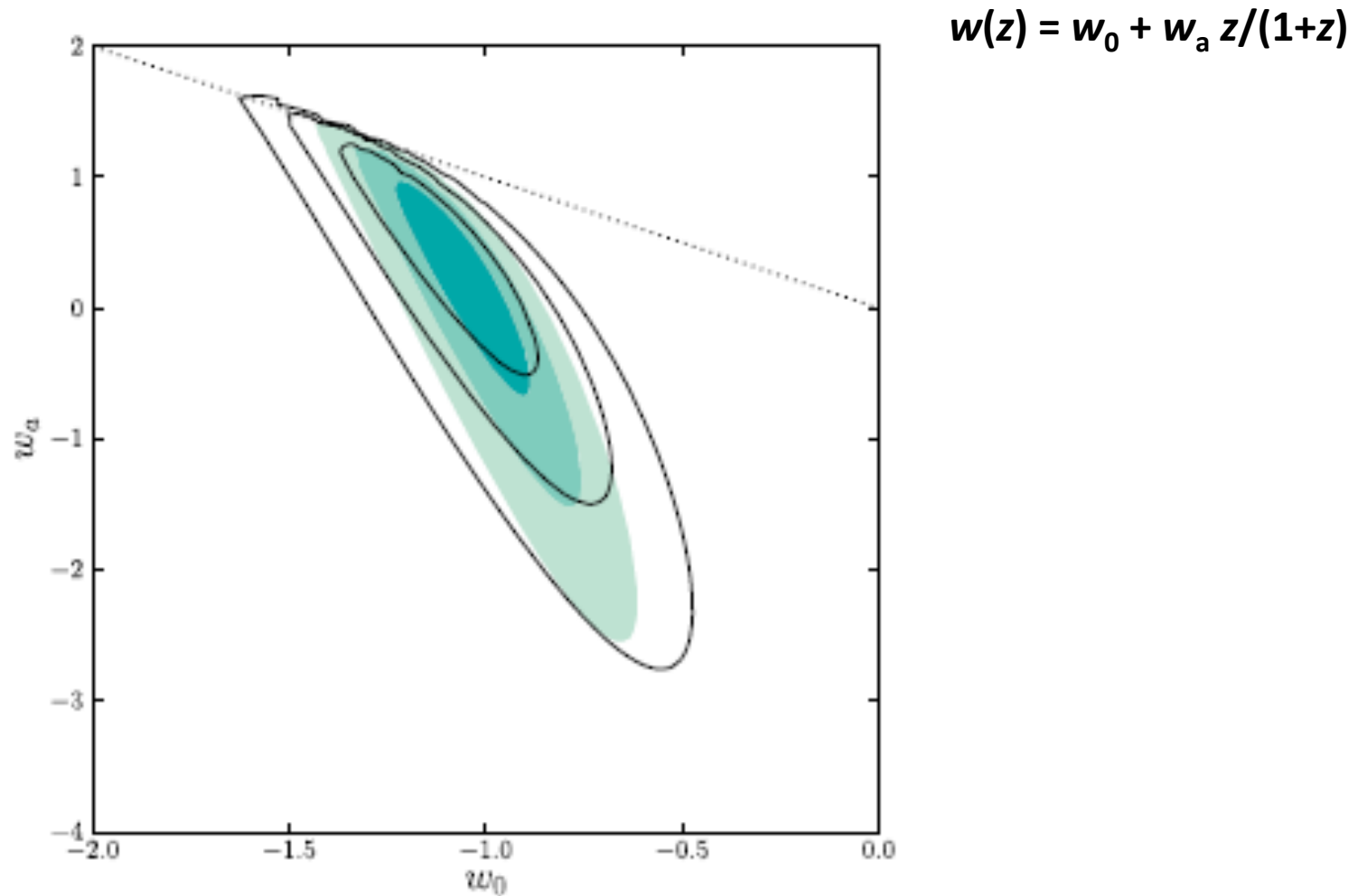


Combined SNIa, CMB and BAO constraints in the (Ω_M, w) plane

$(w \equiv p/\rho ; w = -1$ for vacuum energy)

(Amanullah et al. 2010)

The Discovery of the Acceleration of the Universe



Confidence regions in the (w_0, w_a) plane, combining SNeIa, CMB, and BAO

(Amanullah et al. 2010)

The Discovery of the Acceleration of the Universe

Union2

Fit Results on Cosmological Parameters Ω_M , w , and Ω_k

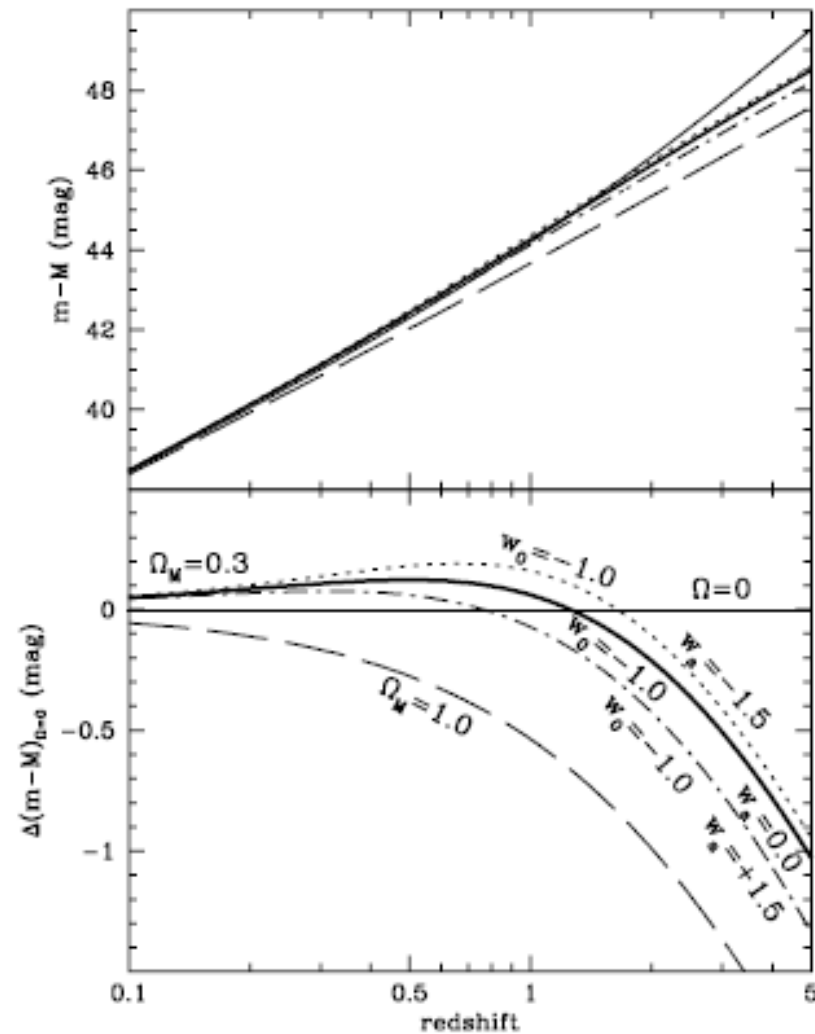
Fit	Ω_M	Ω_M w/Sys	Ω_k	Ω_k w/Sys	w	w w/Sys
SNe	$0.270^{+0.021}_{-0.021}$	$0.274^{+0.040}_{-0.037}$	0 (fixed)	0 (fixed)	-1 (fixed)	-1 (fixed)
SNe+BAO+ H_0	$0.309^{+0.032}_{-0.032}$	$0.316^{+0.036}_{-0.035}$	0 (fixed)	0 (fixed)	$-1.114^{+0.098}_{-0.112}$	$-1.154^{+0.131}_{-0.150}$
SNe+CMB	$0.268^{+0.019}_{-0.017}$	$0.269^{+0.023}_{-0.022}$	0 (fixed)	0 (fixed)	$-0.997^{+0.050}_{-0.055}$	$-0.999^{+0.074}_{-0.079}$
SNe+BAO+CMB	$0.277^{+0.014}_{-0.014}$	$0.279^{+0.017}_{-0.016}$	0 (fixed)	0 (fixed)	$-1.009^{+0.050}_{-0.054}$	$-0.997^{+0.077}_{-0.082}$
SNe+BAO+CMB	$0.278^{+0.014}_{-0.014}$	$0.282^{+0.018}_{-0.016}$	$-0.003^{+0.006}_{-0.006}$	$-0.004^{+0.006}_{-0.007}$	-1 (fixed)	-1 (fixed)
SNe+BAO+CMB	$0.281^{+0.016}_{-0.015}$	$0.282^{+0.018}_{-0.016}$	$-0.004^{+0.007}_{-0.007}$	$-0.005^{+0.008}_{-0.007}$	$-1.029^{+0.056}_{-0.059}$	$-1.038^{+0.093}_{-0.097}$
SNe+BAO+CMB+ H_0	$0.275^{+0.015}_{-0.014}$	$0.274^{+0.016}_{-0.015}$	$-0.001^{+0.006}_{-0.006}$	$-0.002^{+0.007}_{-0.007}$	$-1.024^{+0.055}_{-0.058}$	$-1.052^{+0.092}_{-0.096}$

Note. The parameter values are followed by their statistical (first column) and statistical and systematic (second column) uncertainties.

$w = -0.997 \pm 0.08$ (flat) $w = -1.038 \pm 0.09$ (allowing curvature)

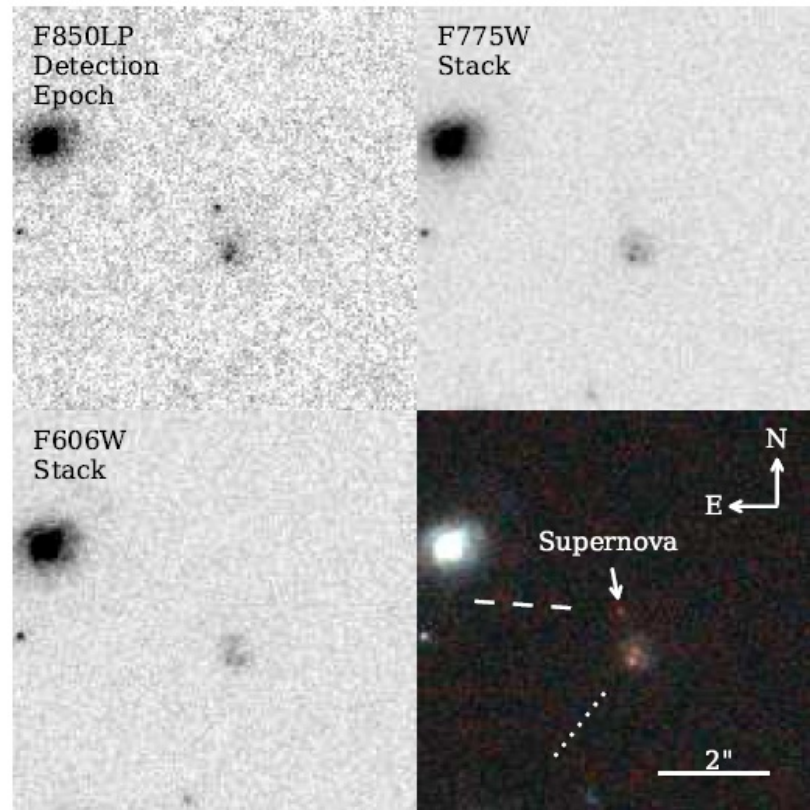
At $z \geq 1$ the existence and nature of dark energy are only weakly constrained by the data

The Discovery of the Acceleration of the Universe



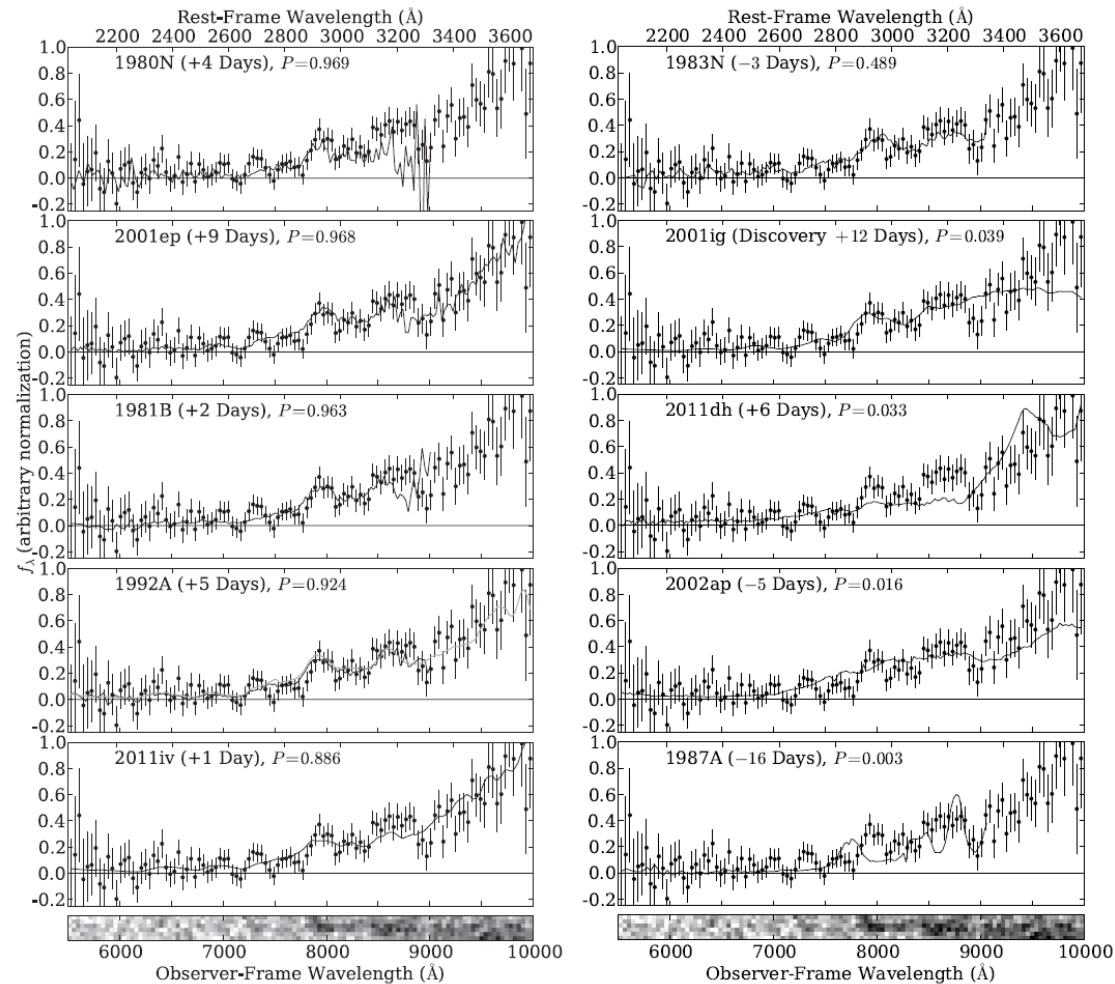
The cosmological constant case (bold line) is compared with evolving models close to $w = -1$, i.e., a model with $w_0 = -1.0$ and $w_a = -1.5$ (short dashed line) and a model with $w_0 = -1.0$ and $w_a +1.5$ (dash-dotted line). Only very accurate measurements will enable to discriminate among different equations of state

Redshift 1.71 supernova



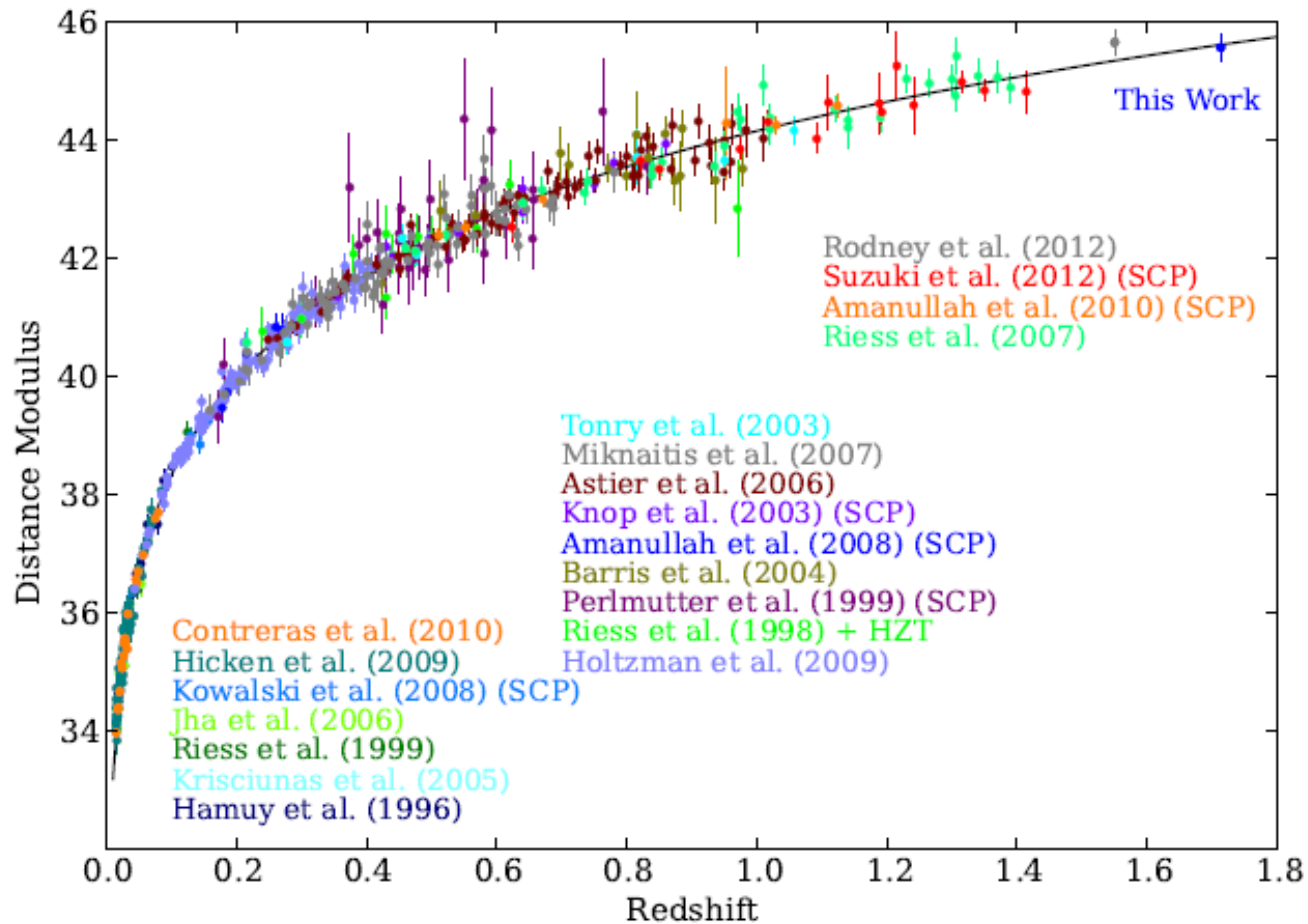
ACS image of the SN location. Lower right panel shows a composite image from the three colors. Lines indicate the dispersion direction in ACS (dashed) and WFC3 (dotted) spectroscopy (Rubin et al. 2013)

Redshift 1.71 supernova



Each panel shows a comparison between SN SCP-0401 and another SN. Best-matching comparison SN Ia in the left panels, best-matching CC SN in the right panels. Best match is for SN1992A. Out of 17 CC SN, only SN1983N is a possible match, but it was 2 mag fainter than any typical SN Ia (Rubin et al. 2013)

Redshift 1.71 supernova

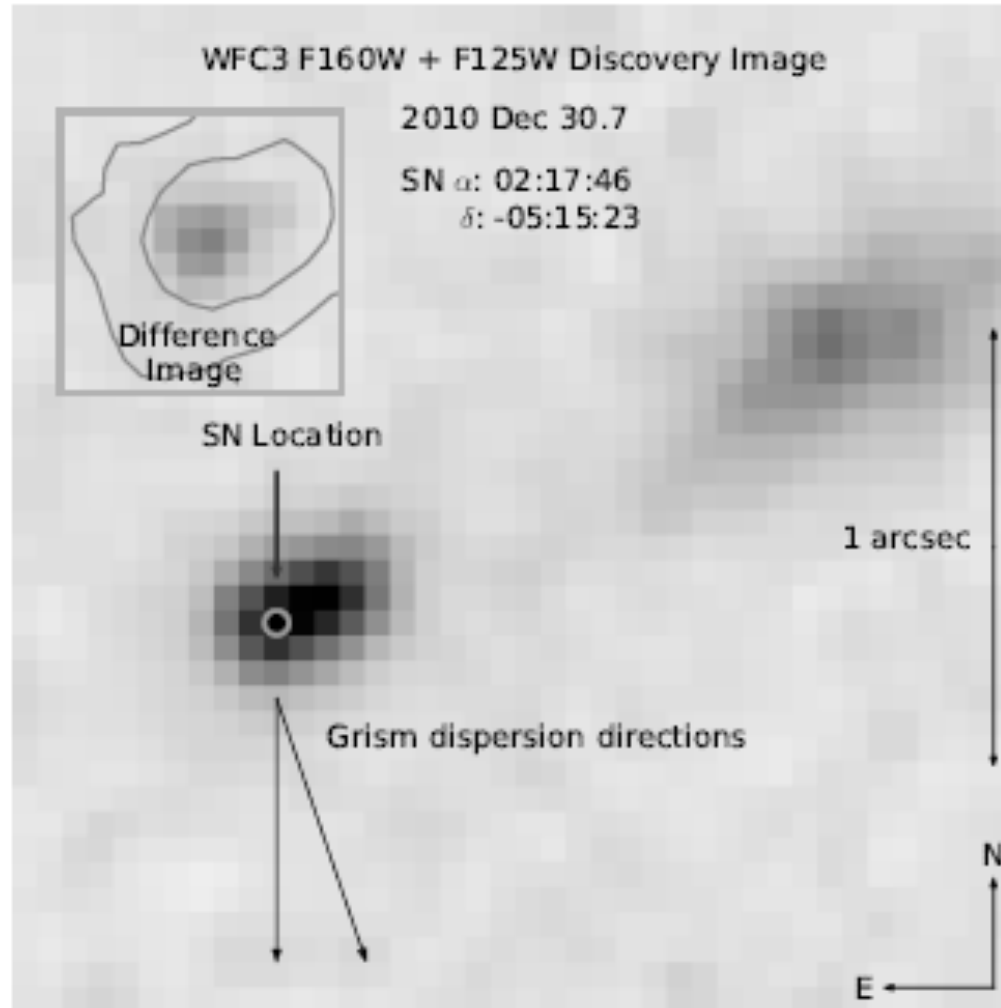


Most recent *SCP* Hubble diagram, with Primo (Rodney et a. 2012) and SCP-0401 SNe added (Rubin et al. 2013)

CANDELS

The Cosmic Assembly Near-IR Deep Extragalactic Legacy Survey, CANDELS ([Grogin et al. 2011](#); [Koekemoer et al. 2011](#)), PI: S. Faber, Co-PI, H. Ferguson, is designed to document the first third of galactic evolution from $z = 8$ to 1.5 via deep imaging of more than 250,000 galaxies with WFC3/IR and ACS. It will also discover and characterize Type Ia SNe beyond $z > 1.5$ and establish their accuracy as standard candles for cosmology

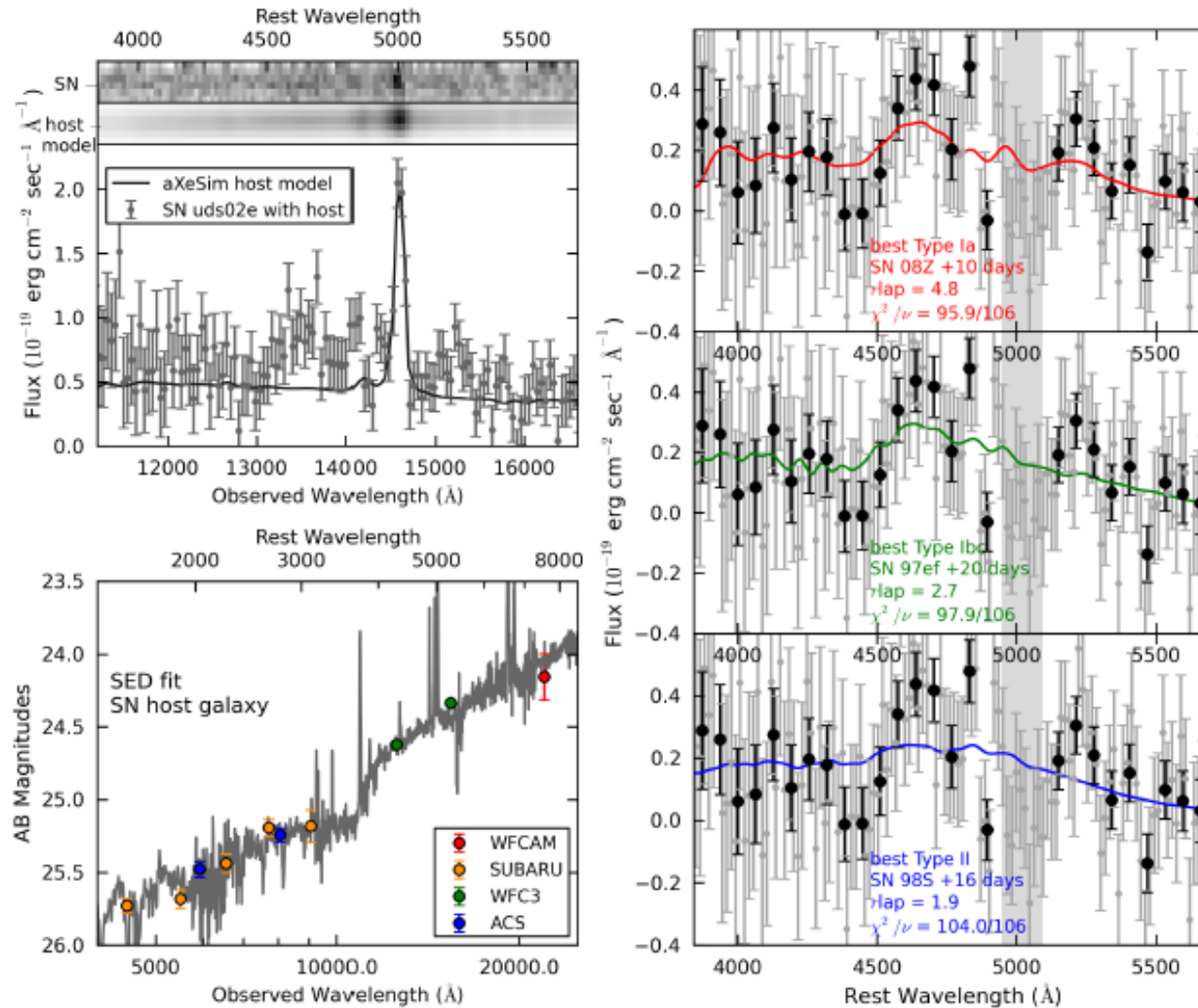
Most distant SN Ia to date



$z = 1.914$

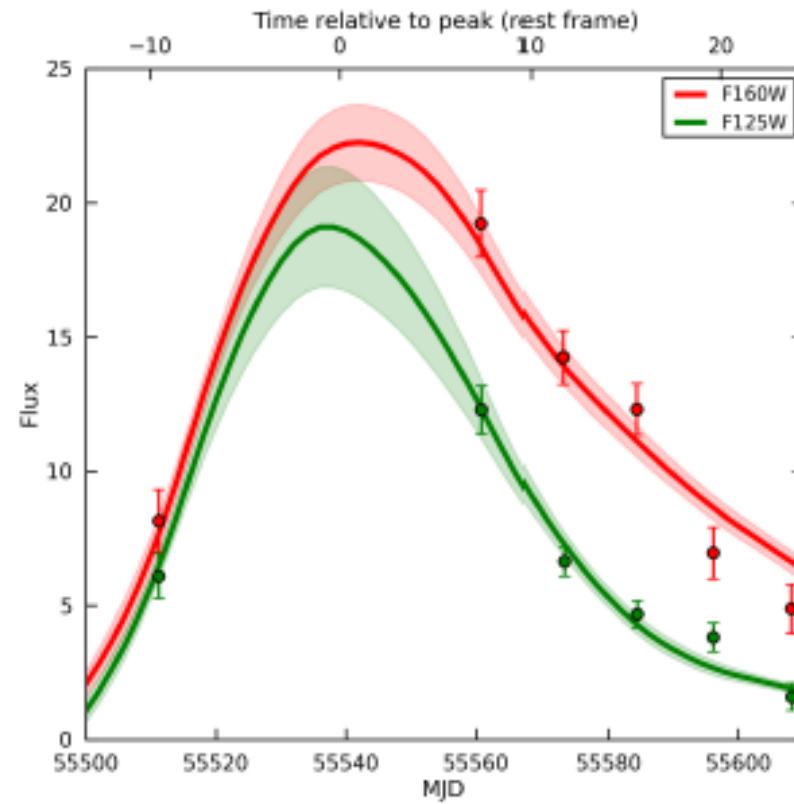
Jones et al.
(2013)

Most distant SN Ia to date



Jones et al.
(2013)

Most distant SN Ia to date



Jones et al.
(2013)

Precision cosmology with SNeIa

Systematic uncertainties:

- **Dust extinction**
- **Possible evolution of the intrinsic properties of SNeIa**

Evidence of two distinct populations of SNeIa hosts: SNeIa in early-type galaxies can be distinguished from those that occur in late-type galaxies

SN Ia and mass of the host galaxy

- The evidence suggests that, after light—curve shape corrections, larger—stellar mass galaxies host the brightest SN Ia.

$$\Delta M_B \approx 0.075 \text{ mag brighter}$$

(Goobar and Leibundgut 2011)

- It is found that SNe Ia in environments with H α emission (star forming regions) are redder by 0.036 ± 0.017 mag. (Rigault et al. 2013).
- SNe Ia associated with local H α emission are more homogeneous, resulting in a brightness dispersion of only 0.105 ± 0.012 mag (Rigault et al. 2013).

SN Ia in progenitor populations

- Currently, using **SALT2.2** to correct for **light curve shape** (x_1 parameter) and **color excess** (c), from the apparent peak blue magnitude m_B , the distance modulus is given by:

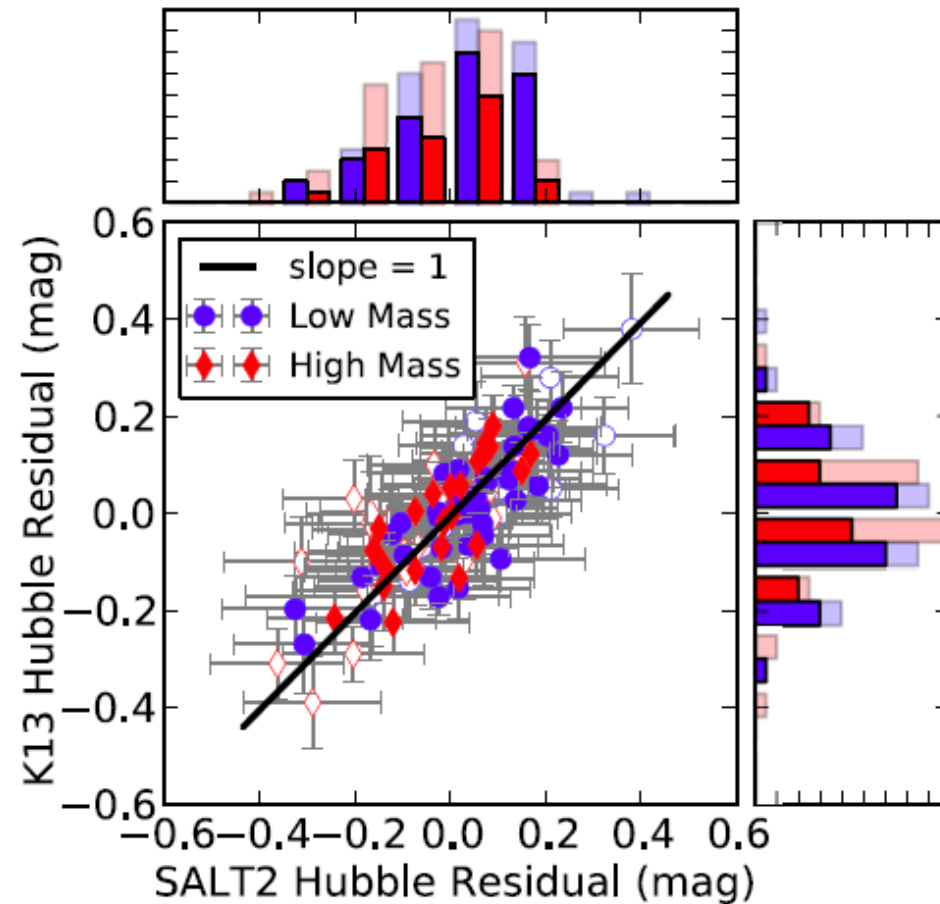
$$\mu_{\text{SN}} = m_B - M_B - \alpha x_1 + \beta c$$

where α , β , and M_B are nuisance parameters determined simultaneously with cosmological parameters. That reduces the scatter of μ_{SN} about the best-fit model to $\approx 15\%$, down from the $\approx 50\%$ scatter for uncorrected absolute peak magnitudes

- Kim et al. (2014) suggest another light-curve fitter **K13**
The brighter supernovae correlated with massive galaxies is only seen as 0.045 ± 0.026 mag effect.
- Need to understand the physics of SN Ia brightness variations and of empirical brightness calibrations and the possible evolution of those calibrations and of SN Ia demographics

Hubble residuals and host galaxy properties

SALT2 vs K13
Hubble
residuals for
a large
sample of
SNeIa from
the *Nearby
Supernova
Factory*



(Kim et al. 2014)

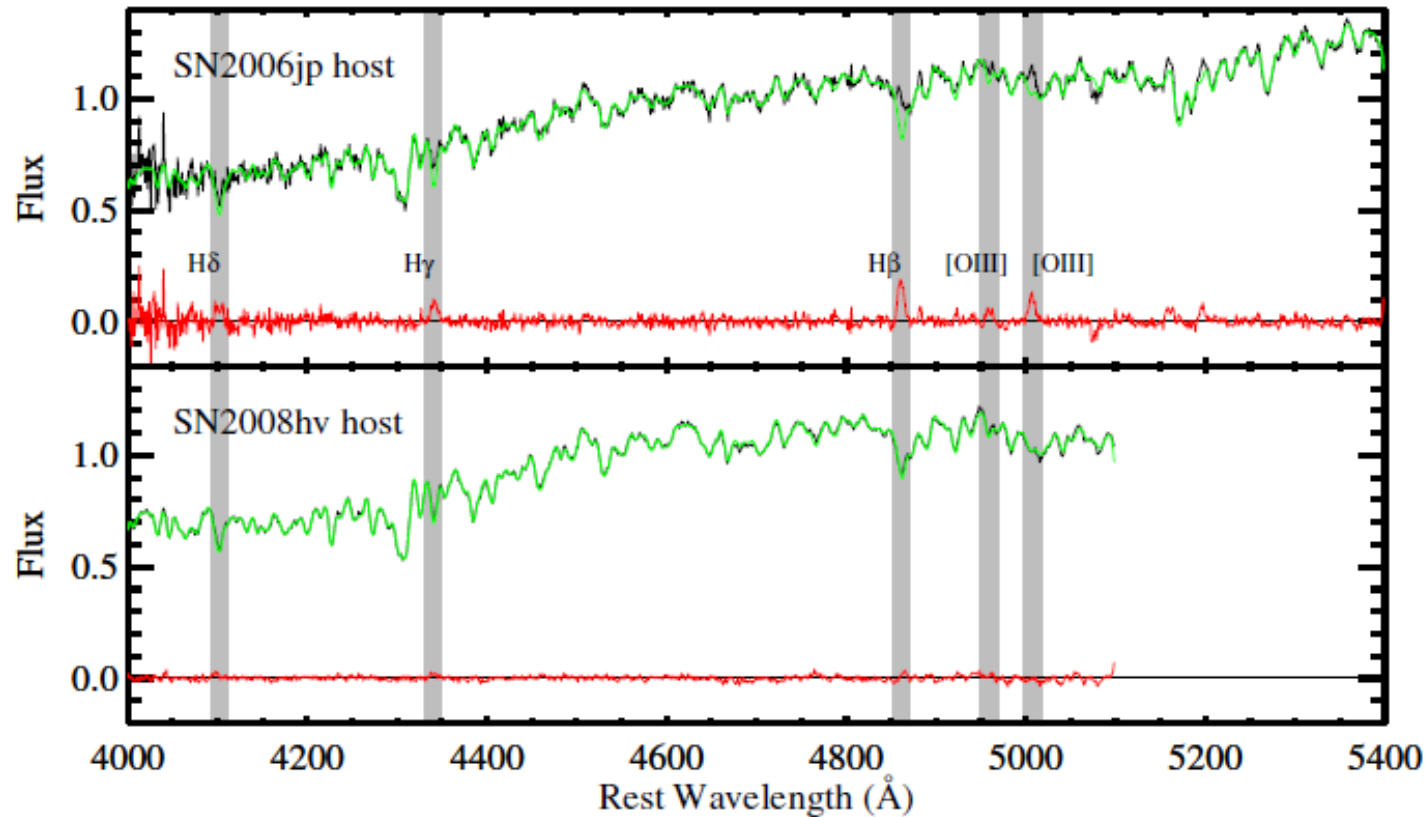
SNela in progenitor populations

- Likely candidates are **progenitor age** and **metallicity** (correlated with the mass in stars and the specific star-formation rates of galaxies)
- Both evolve along the z range probed by SNela, but in distinct ways
- Differences in age or composition of the progenitor white dwarfs may influence SN Ia explosion products and, in particular, the amount of ^{56}Ni produced, which is directly linked to peak luminosity
- Brighter SNela are associated with younger stellar populations. Galaxies having such populations also produce many more SNela per unit stellar mass than galaxies with older stars
- Photometric studies of those correlations are hampered by the age-metallicity degeneracy.
- Absorption line spectroscopic studies, restricted to passively evolving stellar populations, can probe age, metallicity, and even the abundances of some chemical elements

SNela in passive progenitor populations

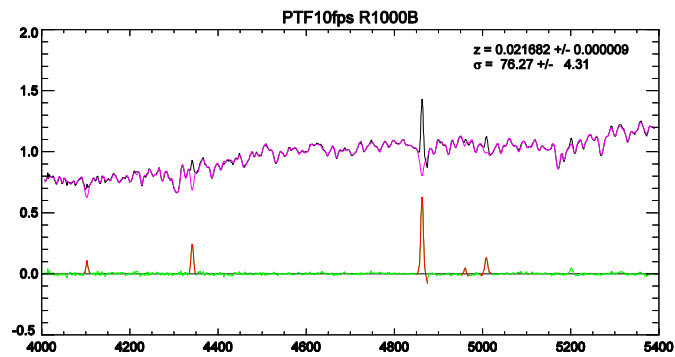
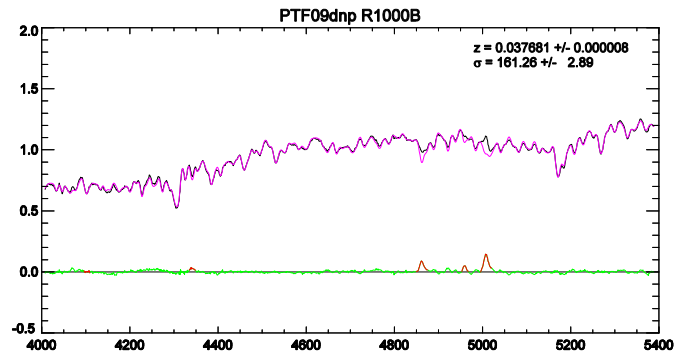
- Spectroscopic survey of 40 passive SNela hosts, at high signal-to-noise ratio, enough to separate age and metallicity constraints
- Obtained constraints on the abundances of individual elements
- Used 10-m class telescopes: Keck-1 (LIRIS) and GTC (OSIRIS)
- Used a program to measure the smearing of the absorption lines attributable to the galaxy's velocity dispersion
- Used the stellar population synthesis code EZ_AGES

SN Ia in passive progenitor populations



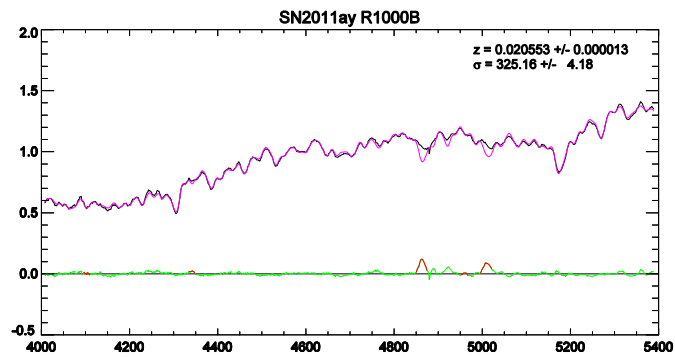
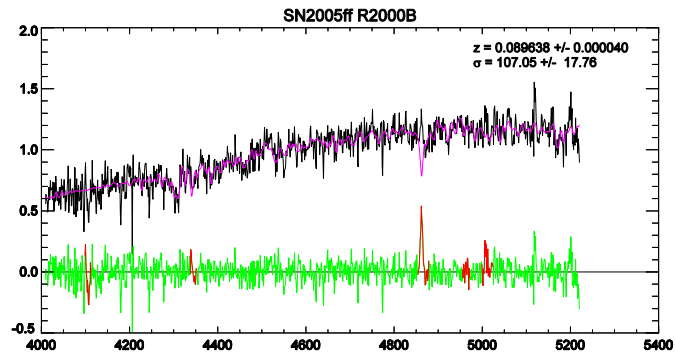
Sample spectra of SN host galaxies. Data are in black, best fits in green, and residuals in red (Meyers et al, incl. PRL and J. Méndez, in preparation, 2013)

SN Ia in passive progenitor populations



Spectra of two SNIa host galaxies, obtained with *OSIRIS* in the *GTC*

SN Ia in passive progenitor populations



Spectra of two SNIa host galaxies, obtained with *OSIRIS* in the *GTC*

SNela in progenitor populations

TABLE 3
FITS TO AGE AND [Fe/H]

Ordinate	Abscissa	slope	P(sign flip)
<i>Fits including SN2005fh</i>			
x_1	log(age)	-2.028 (3.5 σ)	0.00125
x_1	[Fe/H]	5.618 (1.5 σ)	0.06380
color	log(age)	-0.085 (1.0 σ)	0.15355
color	[Fe/H]	1.171 (1.8 σ)	0.03723
HR	log(age)	0.122 (1.0 σ)	0.15677
HR	[Fe/H]	-0.025 (0.0 σ)	0.49335
<i>Fits excluding SN2005fh</i>			
x_1	log(age)	-2.302 (4.7 σ)	0.00000
x_1	[Fe/H]	5.868 (1.8 σ)	0.03228
color	log(age)	-0.069 (0.8 σ)	0.21407
color	[Fe/H]	1.083 (1.7 σ)	0.04610
HR	log(age)	0.137 (1.1 σ)	0.14702
HR	[Fe/H]	-0.194 (0.1 σ)	0.44590

NOTE. — The slope column indicates both the median slope of the posterior distribution returned by LINFIT and in parentheses the significance computed as the median slope divided by half the range of the smallest interval containing 68% of the posterior probability.

TABLE 4
 FITS TO METAL ENHANCEMENTS

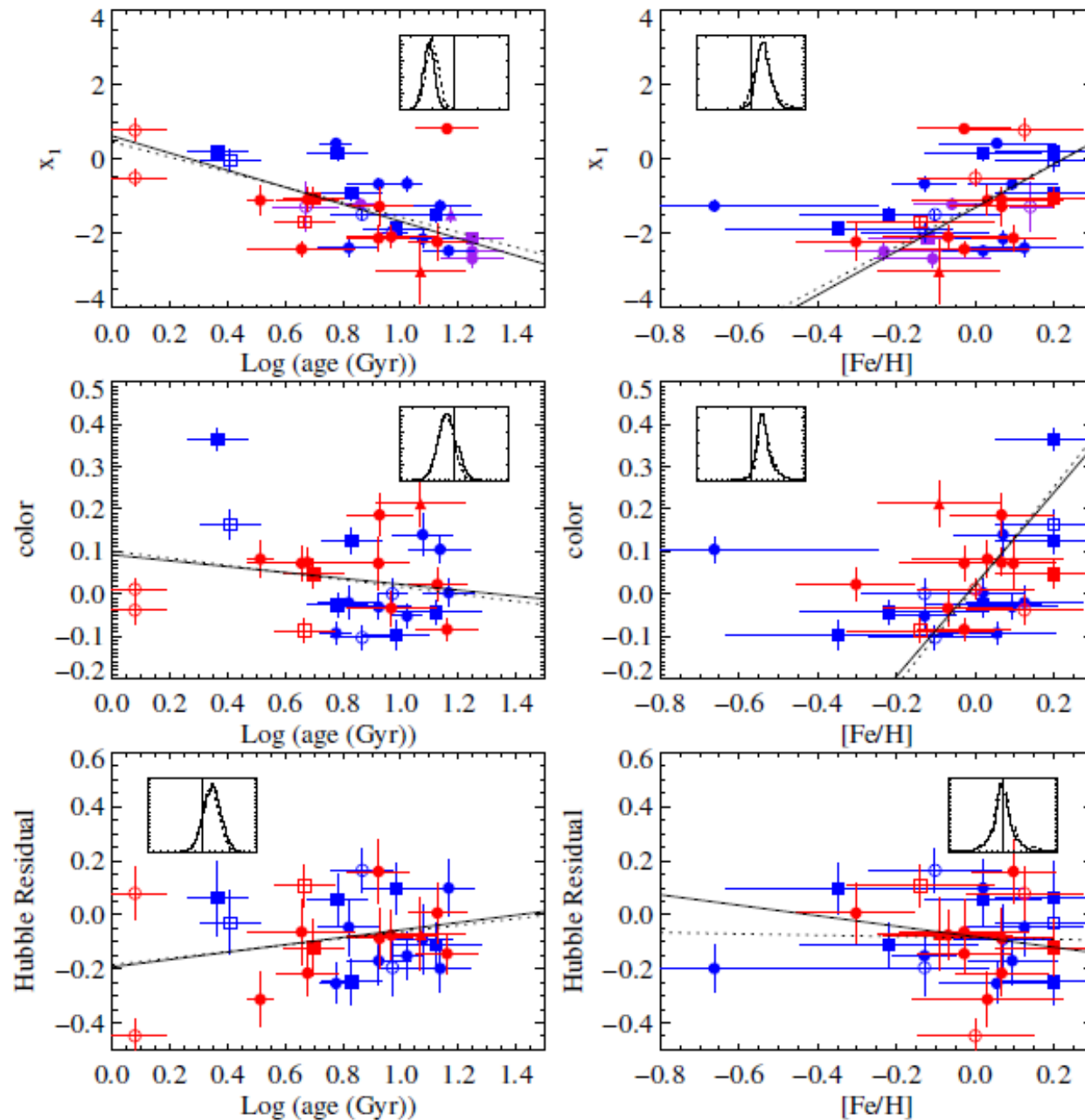
Ordinate	Abscissa	slope	P(sign flip)
<i>Fits including SN2005jh</i>			
x_1	[Mg/Fe]	-2.514 (1.4 σ)	0.07740
x_1	[C/Fe]	2.437 (1.3 σ)	0.08672
x_1	[N/Fe]	-2.020 (2.8 σ)	0.00955
x_1	[Ca/Fe]	-4.582 (0.3 σ)	0.36757
color	[Mg/Fe]	-0.084 (0.4 σ)	0.34767
color	[C/Fe]	-0.088 (0.4 σ)	0.34385
color	[N/Fe]	-0.225 (2.5 σ)	0.01300
color	[Ca/Fe]	-1.391 (0.6 σ)	0.26830
HR	[Mg/Fe]	-0.391 (1.2 σ)	0.13000
HR	[C/Fe]	-0.386 (1.5 σ)	0.09185
HR	[N/Fe]	0.080 (0.5 σ)	0.30905
HR	[Ca/Fe]	-0.434 (0.1 σ)	0.44750
<i>Fits excluding SN2005jh</i>			
x_1	[Mg/Fe]	-1.786 (1.0 σ)	0.15163
x_1	[C/Fe]	5.173 (2.5 σ)	0.00340
x_1	[N/Fe]	-1.885 (2.7 σ)	0.00708
x_1	[Ca/Fe]	-4.104 (0.3 σ)	0.34910
color	[Mg/Fe]	-0.144 (0.6 σ)	0.27138
color	[C/Fe]	-0.261 (0.9 σ)	0.16387
color	[N/Fe]	-0.223 (2.4 σ)	0.01155
color	[Ca/Fe]	-1.531 (0.7 σ)	0.23022
HR	[Mg/Fe]	-0.439 (1.3 σ)	0.10430
HR	[C/Fe]	-0.500 (1.7 σ)	0.06768
HR	[N/Fe]	0.081 (0.5 σ)	0.30867
HR	[Ca/Fe]	-0.311 (0.1 σ)	0.46288

NOTE. — The slope column indicates both the median slope of the posterior distribution returned by LINFIT and in parentheses the significance computed as the median slope divided by half the range of the smallest interval containing 68% of the posterior probability.

SN Ia in progenitor populations

Possible theoretical interpretations:

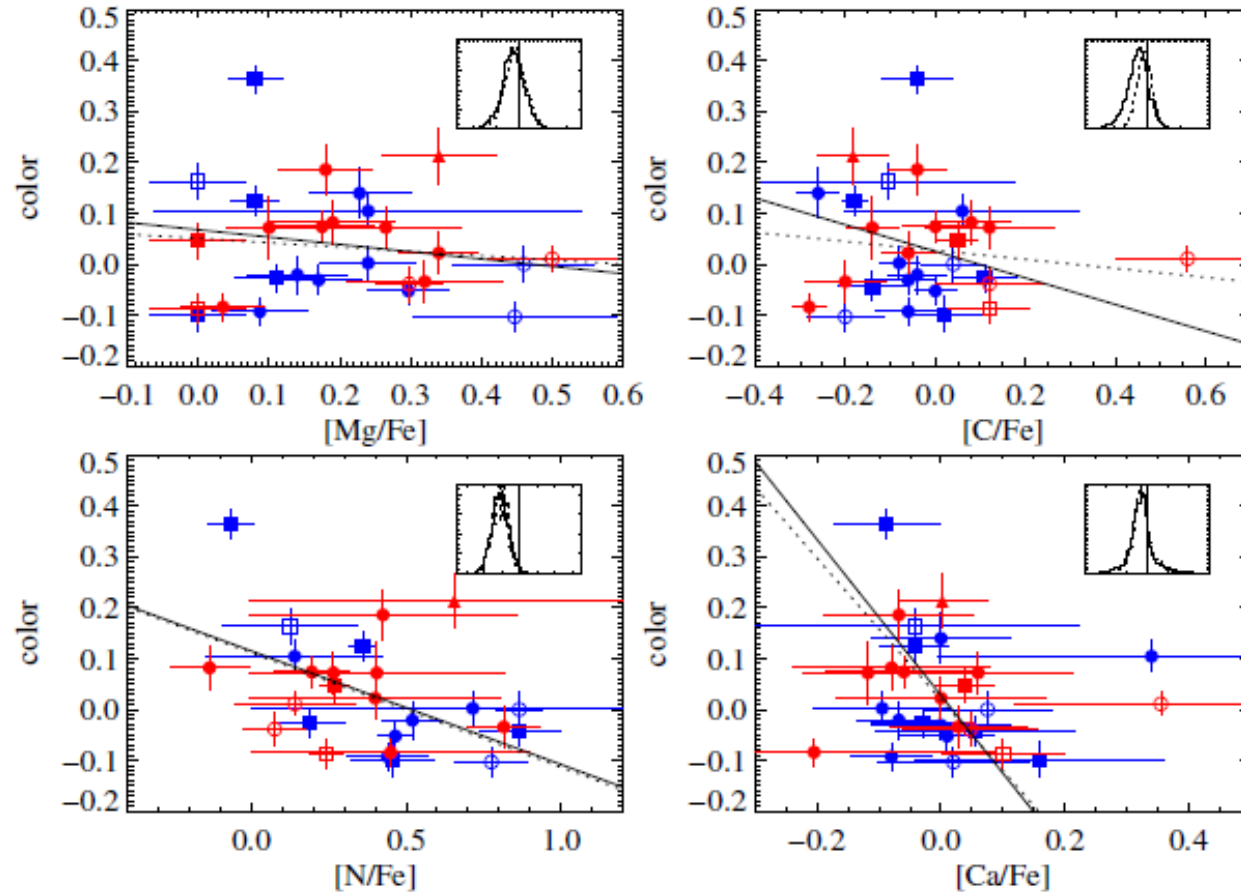
- C mass fraction in C+O white dwarfs is smaller if the stars formed in lower metallicity or older environments. They produce fainter SN Ia (Umeda et al. 1999)
- On the contrary, it has been argued that lower metallicity progenitors should produce more ^{56}Ni . That due to smaller neutron abundances (less ^{22}Ne coming from CNO, at the end of the He-burning phase). However, scatter plots of x_1 against the predicted mass of radioactive Ni do not show any trend. Suggests that neutronization due to metallicity is not the dominant source of x_1 diversity in SN Ia
- A still unexplored point is that older white dwarf progenitors have also been cooling longer. Their interiors have partially crystallized and that should affect the ignition and the initial stages of propagation of the thermonuclear burning



Insets show the posterior probability distribution function for the slope of the linear regression

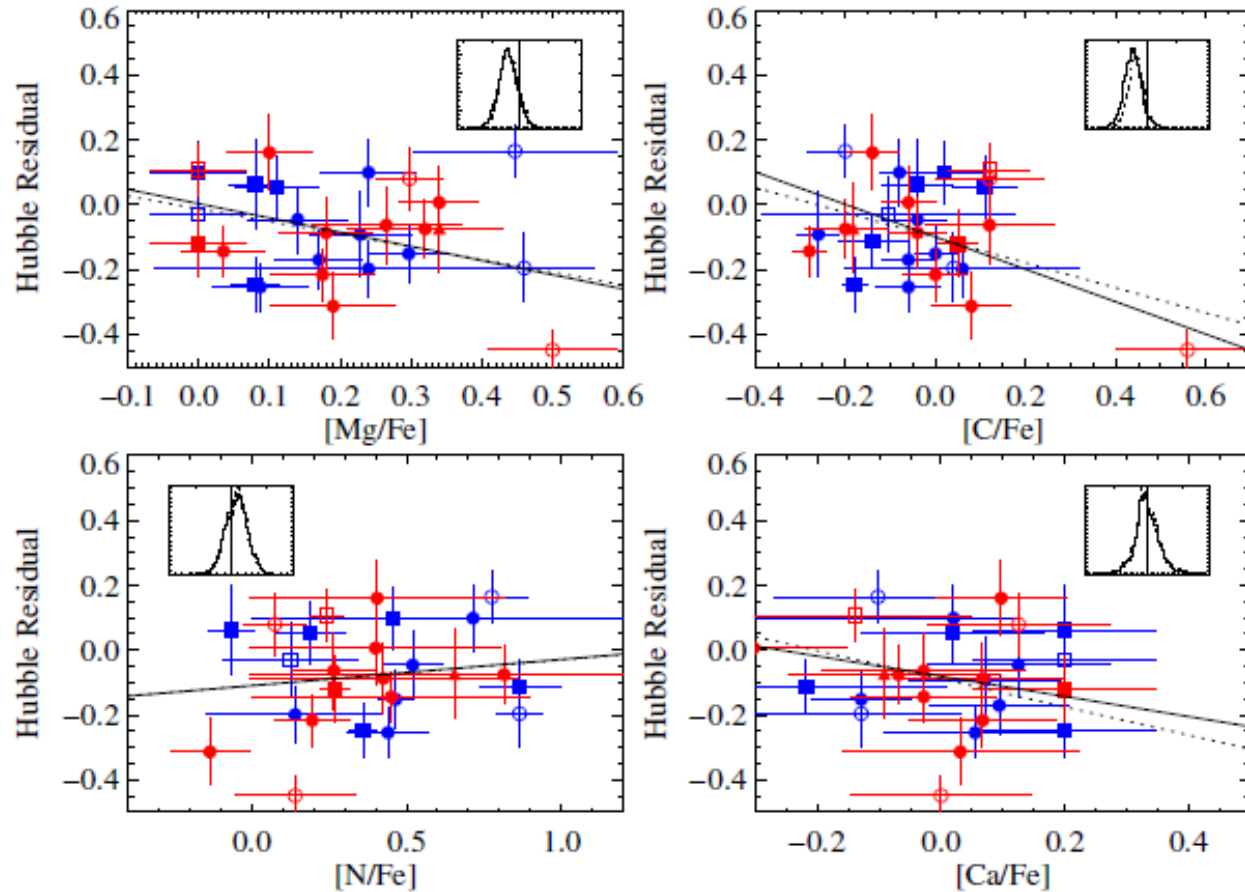
Correlations between age (left) and metallicity (right) of the host galaxies with the SALT2.2 parameters x_1 and c of the SNeIa light curves, and with the Hubble residuals

SNela in passive progenitor populations



The SALT2 colorparameter c plotted against host galaxy metal abundances $[\text{Mg}/\text{Fe}]$, $[\text{C}/\text{Fe}]$, $[\text{N}/\text{Fe}]$, and $[\text{Ca}/\text{Fe}]$

SN Ia in passive progenitor populations



SN Ia Hubble residuals plotted against host galaxy metal abundances $[\text{Mg}/\text{Fe}]$, $[\text{C}/\text{Fe}]$, $[\text{N}/\text{Fe}]$, and $[\text{Ca}/\text{Fe}]$

SN Ia in passive progenitor populations

The strongest correlation between any SN Ia property and host galaxy property is that of the light curve shape parameter x_1 with the log of the host galaxy age. The significance of this trend is 3.5σ , taking the full sample, and 4.7σ if the outlier SN2005fh is removed

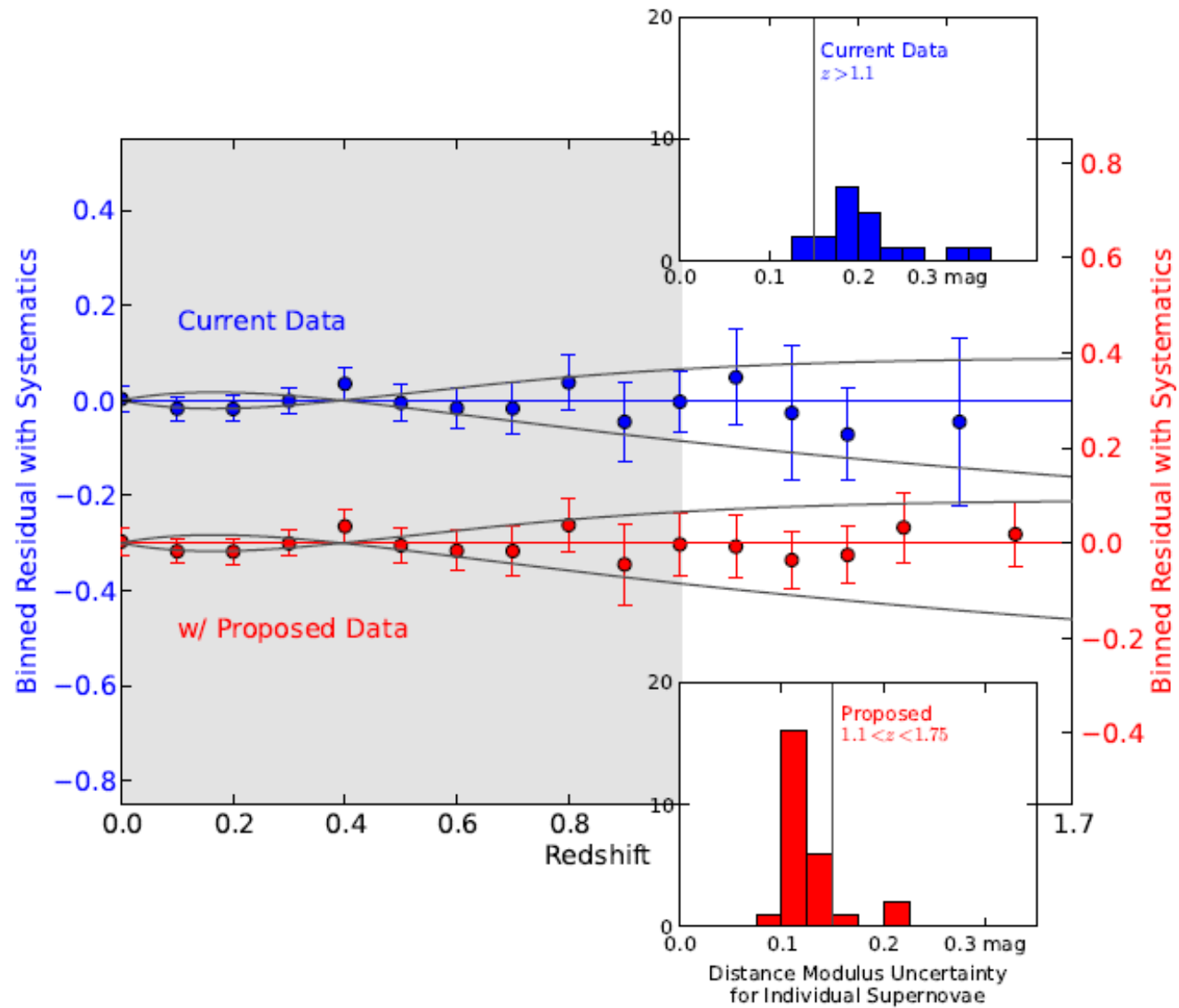
There is also a trend, with significance 1.8σ , between x_1 and [Fe/H]

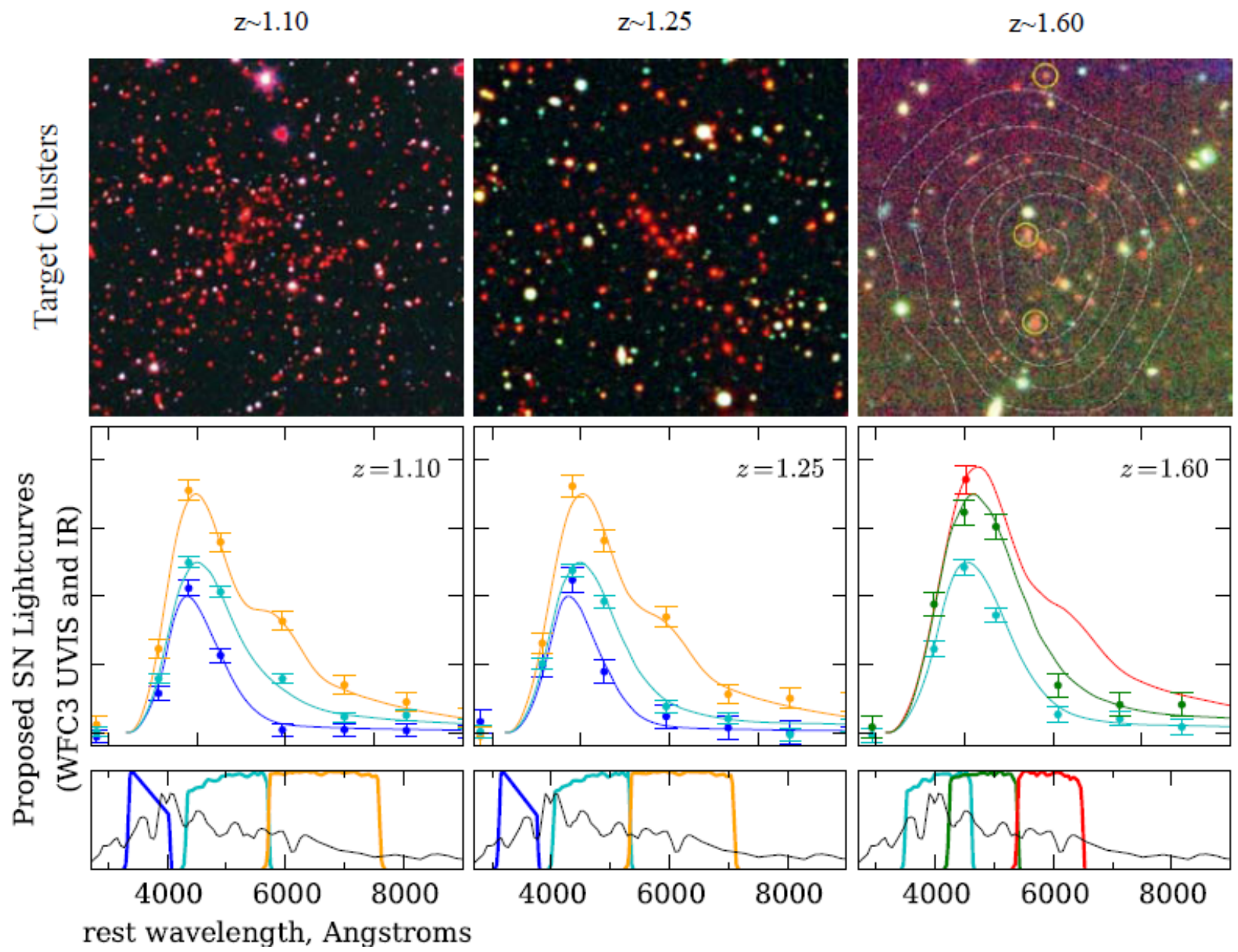
There is a 1.7σ correlation between host galaxy [Fe/H] and SN color, but no correlation with galaxy age

Neither galaxy age nor [Fe/H] appear to influence Hubble residuals.

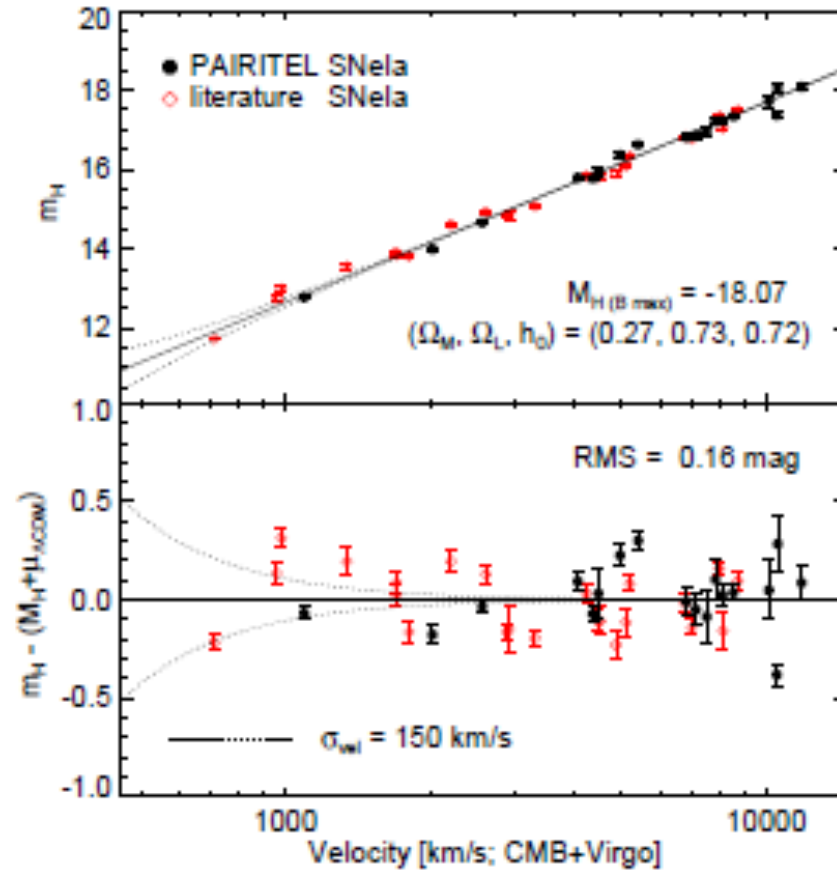
[C/Fe] and {N/Fe} are also correlated with x_1 (2.5σ and 2.7σ , respectively)

SN Ia in high- z galaxy clusters





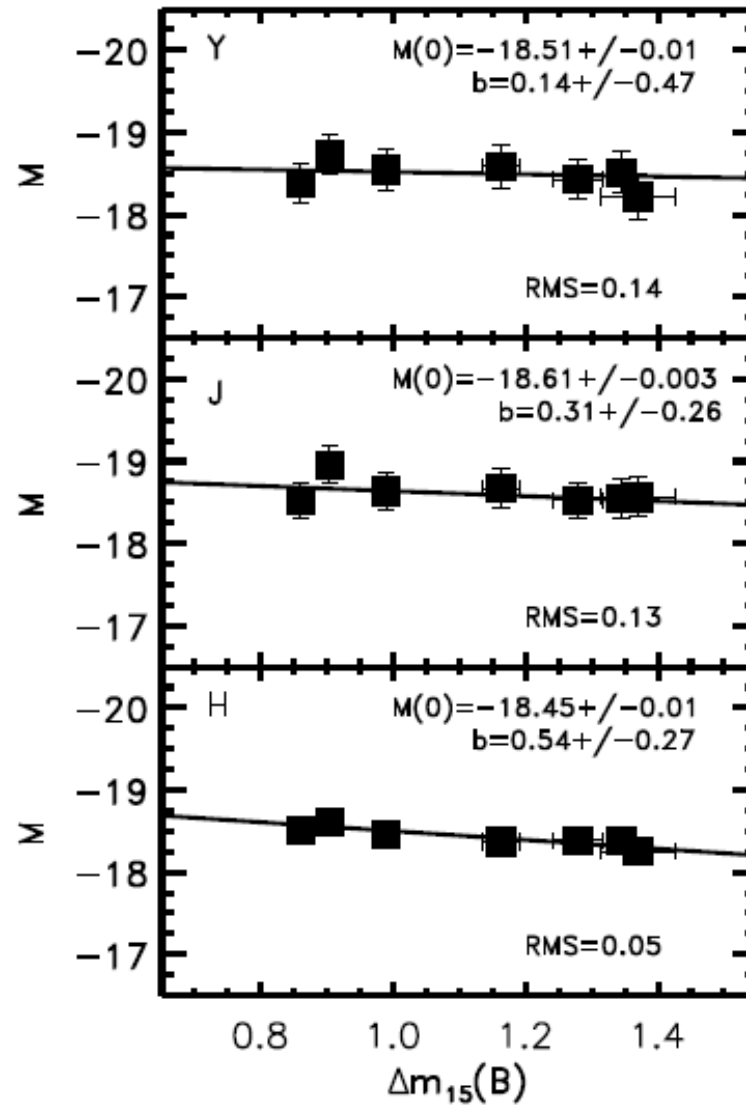
A new proposal



H-band SN Ia Hubble diagram. It includes 23 SN Ia observed with PAIRITEL (Wood-Vasey et al. (2008))

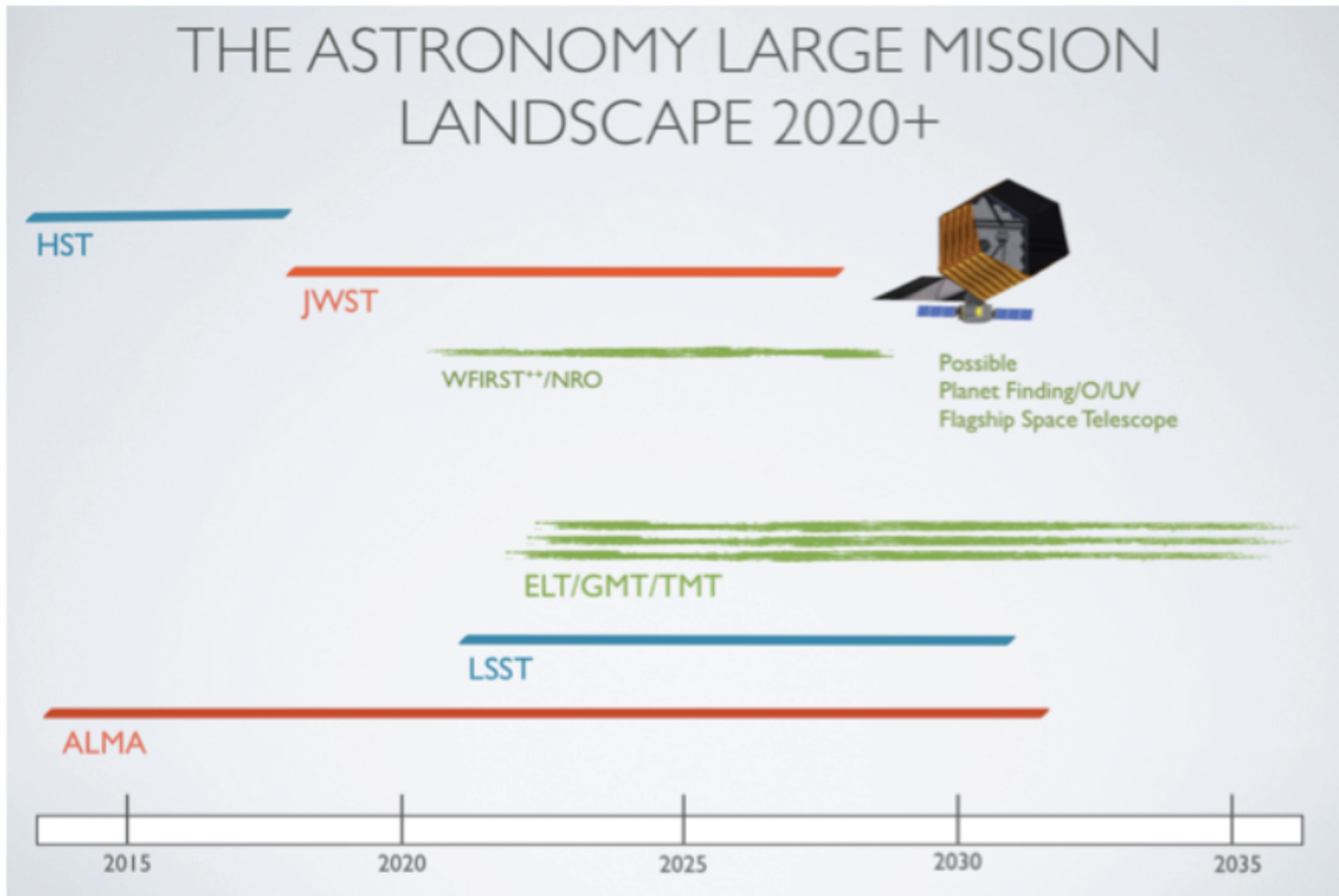
A new proposal

Fits of absolute
YJH magnitude
vs decline rate



(Kattner et al. 2012)

WFIRST



(Dressler et al. 2010)

WFIRST/JWST

- **WFIRST: 2.4m 0.281 sqdeg FOV**

2700 Sne Ia with $z=0.1-1.7$

It goes to 20,000 Å : Classical use in cooperation with ground based telescopes

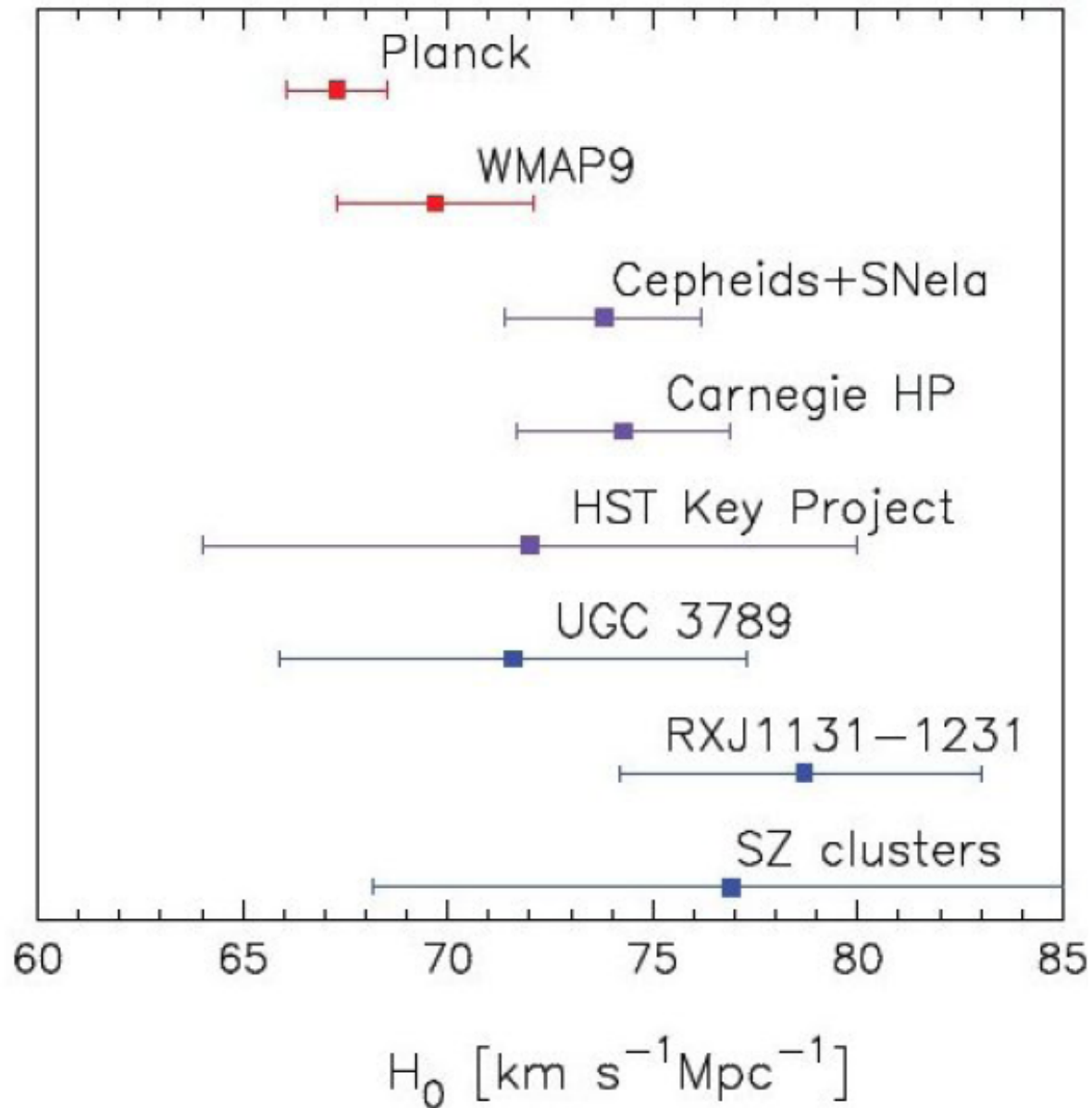
- **JWST: 6.5m 2x2 arcmin FOV**

Sne Ia up to $z=3.5$ with the classical use

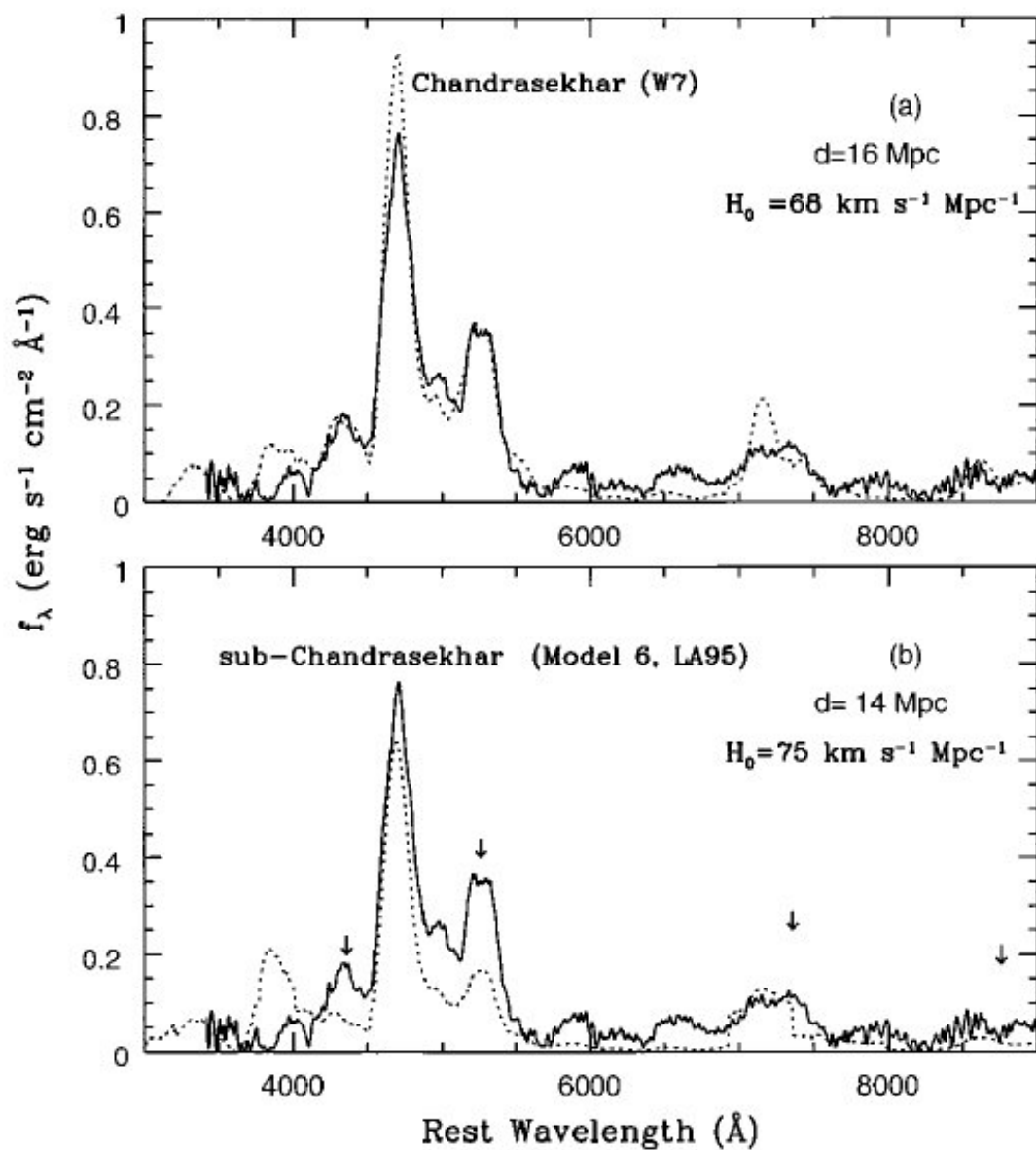
H-band (restframe 15000 Å) infrared candle up to high z

Number of Sne Ia depends on panel.

The Hubble constant



The Hubble constant



PRL (1996)

Conclusions

- We have observed, for the first time, SNela at $z > 1.5$
- The most distant SNela fit the Λ CDM model
- It has been confirmed that SNela with the largest stretches are found in star-forming galaxies
- There is no metallicity dependence of the stretch.
- The above indicates that stretch mainly depends on the ages of the SNela progenitor
- It appears that SNela are better standard candles in the infrared, mild stretch correction being needed there